JOURNAL OF OPTOELECTRONICS AND ADVANCED MATERIALS, Vol. 11, No. 1, January 2009, p. 26 - 33

Transformations in phase-change memory material during thermal cycling

A.A. SHERCHENKOV[a], S.A. KOZYUKHIN[b], E.V. GORSHKOVA[a]
[a]*Institute of Electronic Technology, Moscow, Russian Federation*
[b]*Kurnakov Institute of General and Inorganic Chemistry, RAS, Moscow, Russian Federation*

Phase transformations in bulk $Ge_2Sb_2Te_5$ and its thin films during thermal cycling were studied by differential scanning calorimetry, and thermal properties were determined. Exothermal peaks due to the amorphous-fcc and fcc-hcp phase changes were observed in the thin films in the temperature ranges of 145-190 and 205-230°C, respectively. In addition, reproducible endothermic peak in the range of 390-415°C was revealed in thin films as well as in bulk $Ge_2Sb_2Te_5$, which may influence the kinetics and endurance of writing and erasing processes in phase-change memory devices. Activation energies of observed heat effects were estimated using Kissinger's method, and nature of endothermic peak was discussed.

(Received October 23, 2008; accepted January 21, 2009)

Keywords: Phase-change memory, Chalcogenide alloys, Phase transformations, Differential scanning calorimetry

1. Introduction

Last decade the thin films of chalcogenide alloys have been widely investigated due to their attractiveness as active mediums for optical and electrical memories [1-6]. The work of both types of devices is based on rapid reversible amorphous-to-crystalline phase-change process in nano-volume being initiated by laser or electric impulses. Phase change in such materials is accompanied by a drastic variation in optical and electrical properties [1, 2, 4, 7]. The reversible switching phenomenon was revealed by Ovshinsky [8], which allowed him to use chalcogenide vitreous films for electrical and optical data storage [9, 10].

At present the most widely investigated and used phase-change memory (PCM) materials have compositions along the GeTe-Sb_2Te_3 pseudobinary line, due to the rapid crystallization. The deviation from the line leads to the decrease of the resistivity drop during the crystallization due to the presence of residual amorphous material [11], and increase of the crystallization time [1]. On the other hand, crystallization time monotonically decreases with increasing Sb_2Te_3 content; however amorphous state becomes less stable and amorphous films can swiftly crystallize at room temperature [1]. In a phase equilibrium this system forms three intermetallic compounds: $Ge_2Sb_2Te_5$, $GeSb_2Te_4$ and $GeSb_4Te_7$ (so named GST materials) [12]. The most interesting of them is $Ge_2Sb_2Te_5$, which exhibits appreciable stability at room temperature, high crystallization rate and good reversibility between amorphous and crystalline phases.

Nowadays phase change optical recording devices [CD-RW, DVD-RW, DVDRAM, and Blu-ray Disc (BD)] have obvious commercial success. In addition, phase change electrical memory devices [phase-change random access memory (PRAM)] are considered as a most promising candidate for next generation memories due to non-volatility, low power consumption, fast operation speed, high endurance, extended scalability, low manufacturing cost [4, 13, 14].

Despite of successful commercial application of chalcogenide alloys large investigation work must be carried out to allow a competitive PCM technology to be developed. One of the attractive advantages of phase-change memory in comparison with flash memory is considered to be the cycling endurance. Extremely high reliability of chalcogenide PCM was pointed out in several works. However, a wide range of cycle life was indicated (from 10^5 up to 10^{13} cycles [2, 4, 15-17]). Such a large discrepancy can be explained by a little knowledge about physical processes in phase-change materials during thermal cycling, and a number of factors, which can decrease endurance.

It is known that any disposition towards the phase separation is destructive for cycle life [18]. Compounds along the GeTe-Sb_2Te_3 pseudobinary line ($Ge_2Sb_2Te_5$, $GeSb_2Te_4$ and $GeSb_4Te_7$) do form only one phase, however deviation of the composition leads to the formation of two or three phases [12, 15]. Some processes were indicated in works, which can promote formation of different phases during thermal operations. Experimental results demonstrated that during thermal cycling Te atoms segregate to the grain boundaries in chalcogenide $Ge_2Sb_2Te_5$ films [19], reactivity of the chalcogenide materials can lead to the interaction with various adjacent layers of dielectrics and metals (titanium as electrode materials) at high temperatures [20], the phase-change switching process is accompanied by a significant volume change, which in turn results in large stress switching [19, 21, 22], low melting temperature, high vapor pressure of

Te and mobility of its atoms results in tellurium losses [19]. All these processes concomitant to the multiple repeatable switching operations can lead to phase separation and initiate reliability issue. The problem is complicated by the paradoxical situation, when the structures of amorphous and crystalline switching phases in this ternary system are controversial and not well established [5, 18]. In addition, complex Ge-Sb-Te system has a number of metastable states as a result of different reactions at the high temperatures [23]. Meanwhile, it was predicted that the presence of overcoordinated Te atoms can lead to the phase separation in glasses in Ge-Sb-Te system on a nano-scale during thermal cycling, which accompanies lowering of the average coordination number of tellurium [18]. So, for full realization of the potential of chalcogenide alloys and maximization of cycle life of PCM materials, thermal cycling must be thoroughly investigated.

In this work structural transformations and possible phase separation in bulk $Ge_2Sb_2Te_5$ (GST225) and its thin films were studied during multiple heating and cooling cycles using differential scanning calorimetry (DSC).

2. Experimental

The GST225 thin films were deposited on Si (100) substrates by the thermal evaporation of synthesized material. The basic chamber pressure, temperatures of the evaporator and substrates were 10^{-4} Pa, 630 and 50°C, respectively. Thickness of the films was varied from 500 to 900 nm, and deposition rate was ~3 nm/s.

$Ge_2Sb_2Te_5$ alloy was prepared by the quenching technique, materials (99.999%) were weighed according to their atomic percentage and were sealed in quartz ampoule in a vacuum of $5 \cdot 10^{-3}$ Pa. The ampoule was rocked frequently for 6 h at the maximum temperature 750°C to make the melt homogeneous. The melt was quenched in the switched off furnace.

The samples were characterized by different diagnostic techniques. For X-ray diffraction (XRD) experiments $Cu_{K\alpha}$ radiation (λ=0.15418 nm) was mainly used. Surface morphology and thickness of the films were analyzed by atomic force microscopy (AFM SolverPro NT-MDT).

The composition of the thin films was studied by Rutherford backscattering (RBS) spectroscopy of deuterons with energies E_d = 0.4 and 1 MeV at 135^0 scattering angle, and by SEM JSM-6460LV(*JEOL*) with the energy dispersive x-ray analyzer Inka-Sight (*Oxford*).

Differential scanning calorimetry was carried out with an DSC–50 (Shimadzu) analyzer. Thin films were scraped off from the monocrystalline Si substrates with sapphire spatula. Portions of powder of synthesized bulk material (~30 mg) and thin films (2-4 mg) were pressed and sealed in aluminum pans. Heating rate was varied in the range of 5–70 deg/min. Maximum heating temperature was 630°C, and high-purity nitrogen was used to provide an inert atmosphere of N_2. Weight losses in the temperature range from room temperature to 450°C were estimated by the thermogravimetric analysis (NETZSCH TG209 F1) in inert atmosphere of Ar.

3. Results

As was determined from XRD measurements, the bulk GST225 was a polycrystalline mixture, while as-deposited films had amorphous structure.

RBS spectroscopy allowed to determine the ratio Ge/(Sb+Te), which for the thin films was equal to $[Ge_{0.31}(Sb+Te)_1]$. This value with the accuracy of ±5% correspond to the composition of GST225 compound $[Ge_{0.29}(Sb+Te)_1]$. According to the energy dispersive x-ray analysis deviations of the average composition of as-deposited films (Ge = 24 at.%, Sb = 21 at.%, Te = 55 at.%) all along the substrate did not exceed 1.5 at.%.

Figures 1a and 1b show DSC curves for bulk GST225 and its as-deposited thin film measured with a heating rate of 10 deg/min. There is no heat effect for the bulk sample up to 595°C, above which endothermic peak (with maximum at 624.6°C) due to melting of sample can be seen. On the other hand, a number of heat effects can be observed for the as-deposited thin film sample, and peak temperature of melting is lower (616.4°C).

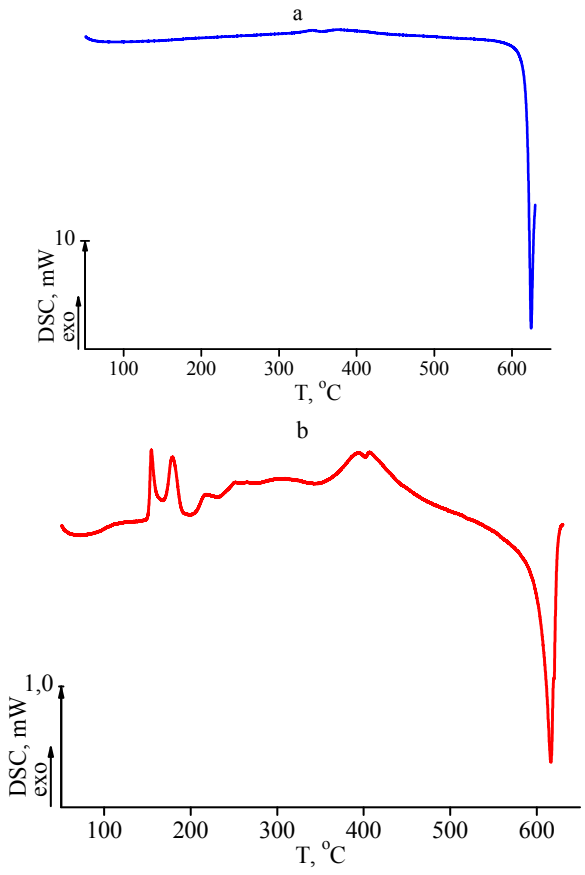

Fig. 1. DSC curves for bulk GST225 (a) and as-deposited thin film (b)

Results of thermogravimetric analysis (Fig. 2) indicates that mass losses in bulk GST225 did not exceed

1% with heating, up to the temperature of 450°C. The losses were two times higher for thin film. However, weighing of the samples after the DSC measurements showed that at higher temperatures the mass losses are much more noticeable, which correlates with the data of work [24]. In this work authors connected the mass losses with the evaporation of Te.

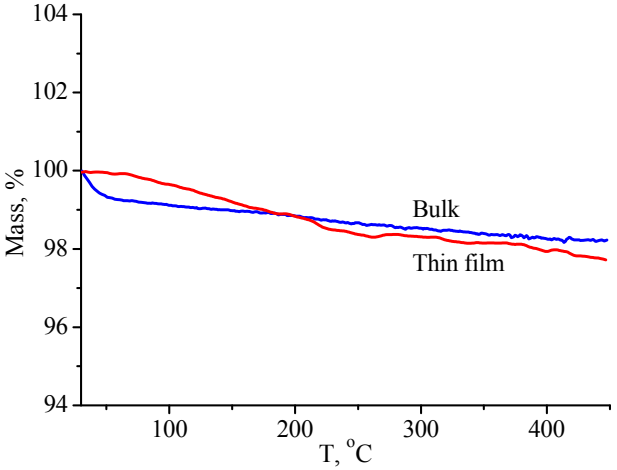

Fig. 2. Thermogravimetric analysis of bulk GST225 and as-deposited thin film.

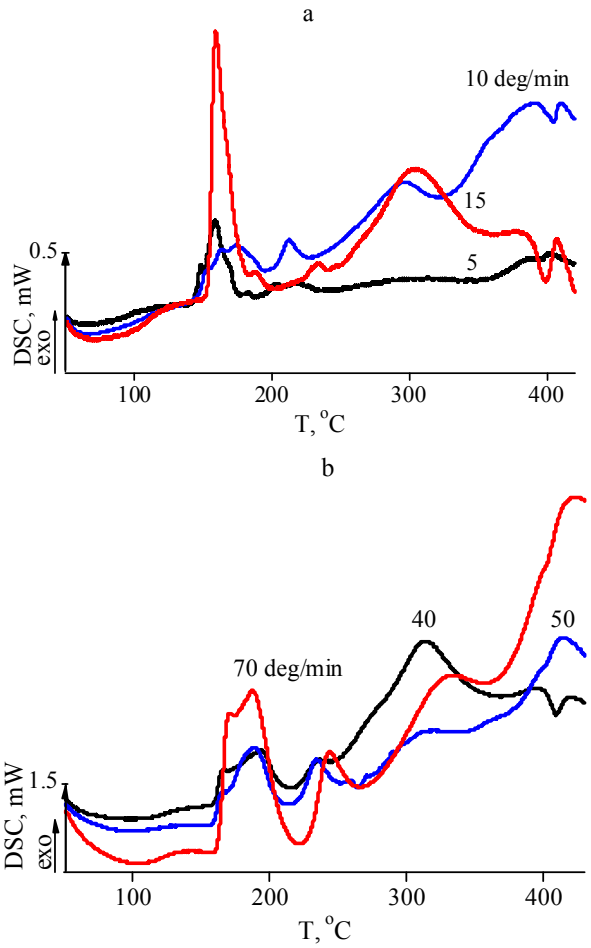

Fig. 3. DSC curves of as-deposited samples obtained at low (a) and high (b) heating rates.

Fig. 3 shows DSC curves of as-deposited samples obtained at different heating rates. With the increase of heating rate peaks of heat effects shift to the higher temperatures and best correlation between DSC curves can be seen if they are divided into two parts: low and high heating rates, such as 5-15 deg/min (Fig. 3a) and 40-70 deg/min (Fig. 3b), respectively. DSC curve measured at 20 deg/min was determined as intermediate.

Despite of some differences in the DSC curves of as-deposited samples obtained at different heating rates (see Fig. 3) the following common features were pointed out:

1) intensive wide and complex exothermic peak in the temperature range 145-190°C is attributed to the transition from amorphous to metastable fcc NaCl type structure;

2) less intensive exothermic peak in the temperature range 205-230°C is attributed to the transition from metastable fcc to the stable hcp phase;

3) wide exothermic peak in the temperature range 250-330°C;

4) endothermic peak in the temperature range 390-415°C.

The nature of two last peaks is not clear. The temperature range of amorphous-fcc transition determined by DSC is in agreement with the results obtained by our measurements of temperature dependence of resistivity for GST225 thin films (Fig. 4) and in the works [17, 19, 25].

The heating is accompanied by the resistivity drop on 3 orders of magnitude. Estimated activation energy for the resistivity is E_a = 0.33 eV, that correlates with the data in [26].

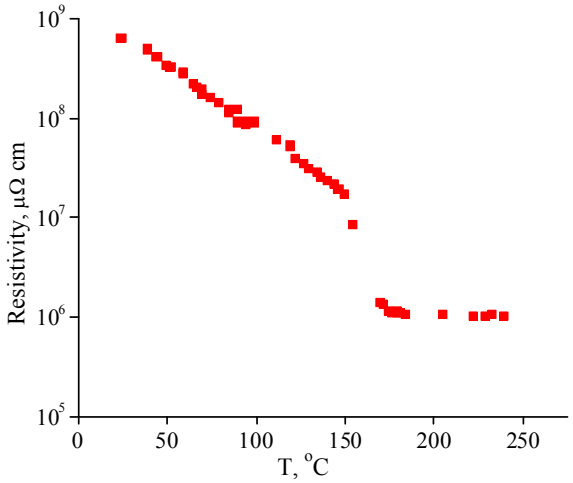

Fig. 4. Temperature dependence of resistivity of GST225 thin film

To elucidate possible morphology changes during the thermal cycling of writing and erasing operations in PCM we investigated by atomic-force microscopy thin films annealed at different temperatures in air during 15 min and these data are shown in Fig. 5. The annealing temperatures were chosen taking into account DSC measurements.

AFM data indicated sharp modification of morphology with the increase of annealing temperature. As-deposited films had an island-like structure with the mean height of ~1 nm (see inset in Fig. 5h).

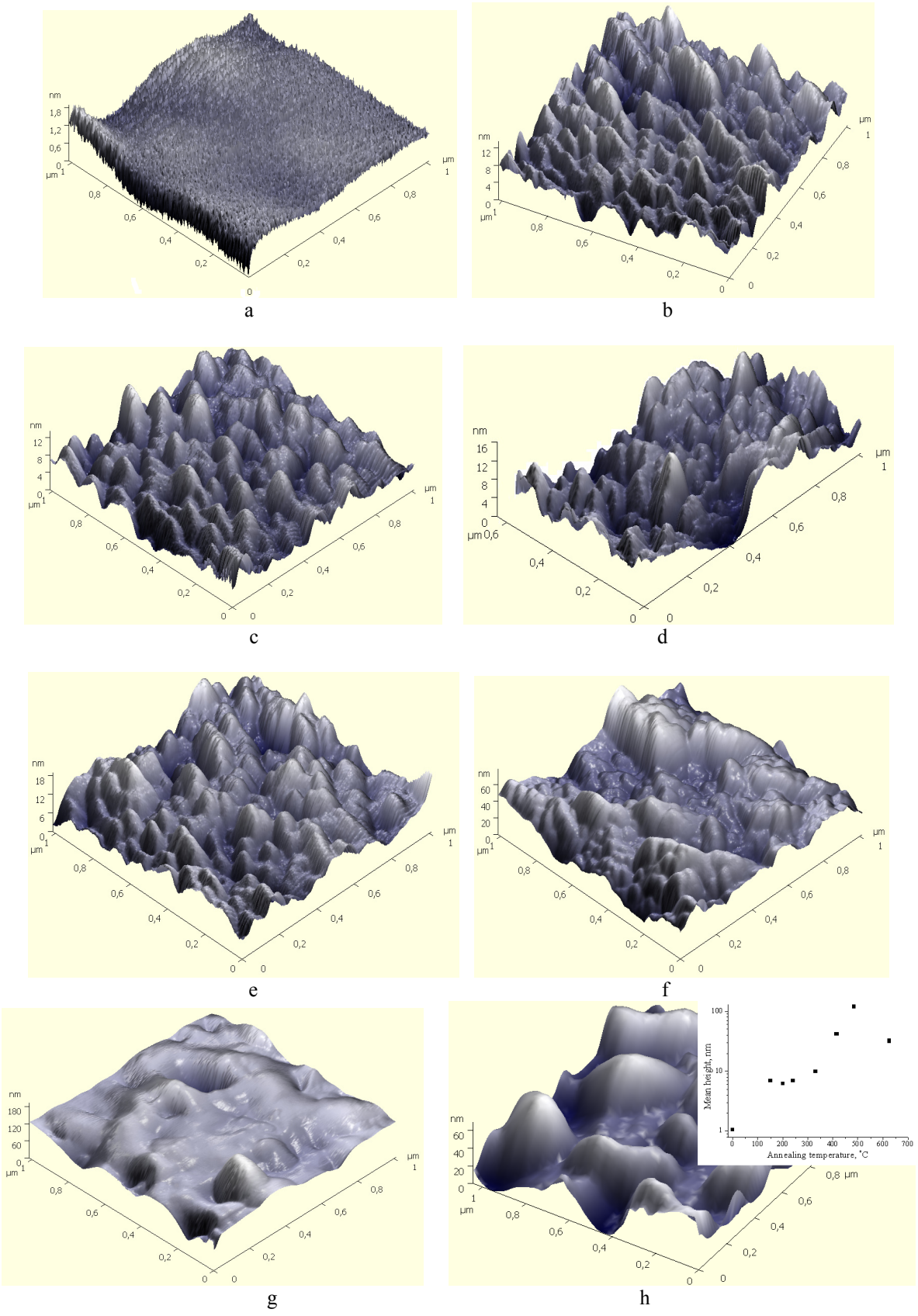

Fig. 5. AFM images of thin films annealed at different temperatures: (a) as deposited; (b) 150 ℃; (c) 200 ℃; (d) 240 ℃; (e) 330 ℃; (f) 415 ℃; (g) 485 ℃; (h) 625 ℃. The inset in (h) shows the dependence of mean height of morphology for GST225 thin film on annealing temperature.

So, thermal cycling in phase change materials can be accompanied by drastic morphology reconstruction.

The influence of the multiple heating and cooling on the phase transformations in bulk and thin film samples were investigated by differential scanning calorimetry. Fig. 6 shows the DSC curves after each repeated DSC experiment. The second DSC measurement of as-deposited film sample leads to the disappearance of the most thermal peaks except for endothermic peak in the temperature range 390-415°C. For the bulk material endothermic peak appeared after the third scanning.

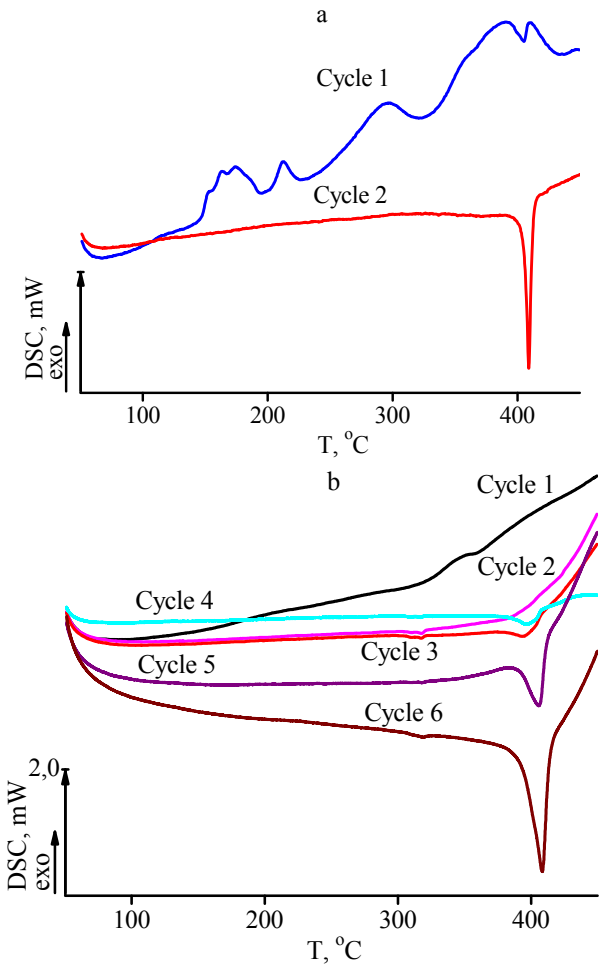

Fig. 6. Repeated DSC curves for thin film (a) and bulk GST225 (b).

4. Discussion

So, DSC measurements indicated that bulk GST225 was in equilibrium state, while as-deposited amorphous films had a number of metastable states. Following DSC measurements of the same thin film sample showed that the value of endothermic peak had sharply increased up to the third scanning, after which slowing was observed (see Fig.7). For the bulk GST225 this peak became noticeable only after the third scanning, and then steadily increased. This difference in the kinetics of the endothermic peak growth for bulk GST225 and thin films can be attributed to the difference in the grains size, which is larger in bulk samples.

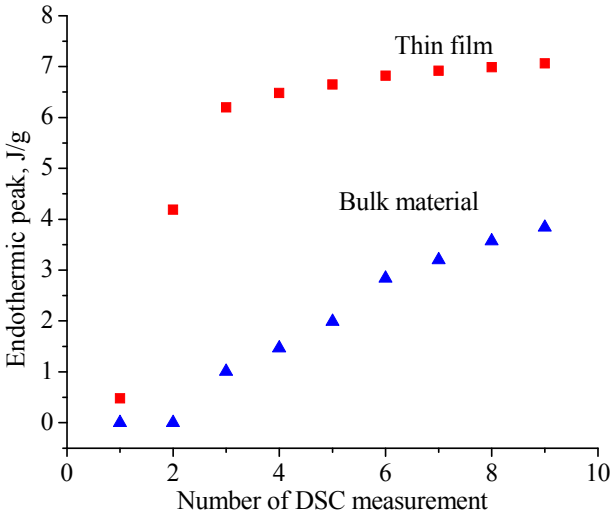

Fig. 7. Dependence of value of the endothermic peak on the number of DSC measurement

All observed effects have thermally activated nature, and we used the Kissinger's method [27] to determine the corresponding activation energies (E_a). This method is based on the relation between peak temperature (T_p) and heating rate (dT/dt)

$$\ln[(dT/dt)/T_p^2] = C + E_a/k_B T_p),$$

where C is the constant and k_B is the Boltzmann constant. Kissinger's plots of $\ln[(dT/dt)/T_p^2]$ vs. $1/T_p$ for as-deposited (amorphous-fcc and fcc-hcp transitions, and endothermic peak in the temperature range 145-190°C) and bulk GST225 (endothermic peak in the temperature range 145-190°C) samples are presented in Fig.8. Each plot was linear fitted, and from the slope $k = E_a/k_B$ activation energy was estimated.

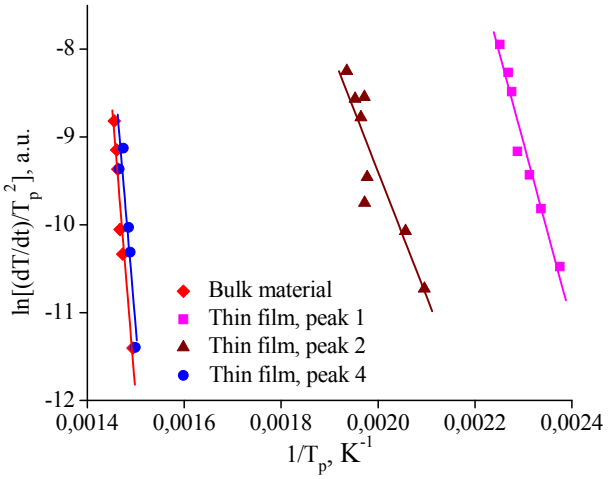

Fig. 8. Kissinger's plots for observed heat peaks on DSC curves.

The results of DSC measurements at heating rate of 10 deg/min are shown in Table 1. Data obtained by other authors are also presented.

It is seen from the table that the data are strongly deviated from each other, and further investigations of thermal properties of GST225 must be carried out. Our value of activation energy for amorphous-fcc transition is smaller than in the works [1,7]. The difference for the activation energy of fcc-hcp transition is larger. This discrepancy can be attributed to the different methods of film deposition and estimation of the activation energy. The values of activation energies for the endothermic peak for bulk GST225 and as-deposited samples are close to each other, and much higher than that for amorphous-fcc and fcc-hcp transitions.

Table 1. Thermal properties of GST225

Sample	Peak type	Temperature range, °C	Peak, °C	Nature	Heat effect, J/g	E_a, eV
Bulk	Endo	390 – 415	395	Melting of $Ge_{18}Te_{82}$ eutectic composition		5.79
	Endo		624,6 630 [12]	Melting of GST225		
Thin film	Exo	145 – 190 100 – 280 ± 30 [25]	154.9 140 [7] 142 [1] 150.8 [19] 153 [17] 154.3 [28] 155.1 [25] 160 [29] 172.7 [30]	Amorphous → metastable fcc	11.58 (11.89 kJ/mol) 0.95±30 kJ/mol [25] 6.07 [17] 16.2±0.5 [19]	1.77 2.23 [1] 2.24±0.11 [7] 2.31 [28]
	Exo	205 – 230	213.1 200 [1] 200 [25] 256.9 [19] 310 [7] 365.3 [30]	Metastable fcc → stable hcp	2.68 (2.75 kJ/mol) 1.80±70 kJ/mol [25] 4.6±0.5 [19]	1.22 3.64±0.19 [7]
	Exo	250 – 330	298.3	Metastable transition	13.51	1.67
	Endo	390 – 415	405.3	Melting of $Ge_{18}Te_{82}$ eutectic composition		5.57
	Endo	610 – 638 [25]	616,4 615.0 [28] 616 [1] 618.6 [30] 621 [25]	Melting of GST225	14.7 ± 7 kJ/mol [25]	

Clarification of the nature of endothermic peak is very important due to its repeatability and possible influence on kinetics and endurance of writing and erasing processes. The existence of endothermic peak near 400°C was observed also in the work [24]. Authors connect its appearance with the agglomeration of Te atoms in the matrix, which follows from the TEM data. In the work [17] decrease and disappearance of fcc GST225 peak with heat treatment at temperatures between 400 and 500°C as well as suppression of the hcp phase were observed by x-ray diffraction. Authors explain these results by the high thermal energy of Te atoms at temperatures above 400°C, which is sufficient enough to allow their segregation to interfaces and a consequent change in stoichiometry to $Ge_2Sb_{2-y}Te_{5-x}$. Furthermore, according to the investigations by TEM with an energy dispersive X-ray analysis [20] mobile Te can easily aggregate at the initially less dense grain boundaries, leaving tiny voids behind and promoting a post-transition stress release even at fairly low temperatures (200°C). Such a diffusion of Te atoms leads to the strong inhomogeneity of the composition of crystalline grains, and can promote phase separation. In this case endothermic peak on our DSC curves resulted from the local melting of different phases. Agglomeration process is connected with the long-distance diffusion of Te atoms and must have large activation energy, which correlates with our DSC data.

Local melting can explain agglomeration of the powder of our thin film samples after the DSC measurements. Examination of the samples also showed the absence of the interaction of powder with the aluminum pans.

Analysis of phase diagrams allows supposing that endothermic peaks are caused by the melting of eutectic compositions. In the work [31] EXAFS results showed that GST225 can include units of Ge_2Te_3, $Ge_{17}Te_{83}$, and

Sb_2Te_3. In the Te-Sb_2Te_3 system eutectic composition with ~11 at.% Sb have melting temperature of 420°C [32], while in the Ge-Te system eutectic composition with ~15 at.% Ge have melting temperature of 375°C [33].

From our point of view the most probable is melting of $Ge_{18}Te_{82}$ eutectic mixture. Assumption of the melting of different eutectic compositions is supported by the character of transformation of endothermic peak during DSC experiments observed for one of our sample. We observed splitting of the peak after multiple measurements (Fig.9). This sample differs from others in that first measurements were carried out up to the temperature of 550°C, which can cause phase separation.

5. Conclusions

Structural transformations and possible phase separation in bulk $Ge_2Sb_2Te_5$ and thin films on its basis during thermal cycling were investigated. Differential scanning calorimetry showed that bulk GST225 material was in equilibrium state, while as-deposited amorphous films had a number of metastable states. Exothermic peaks due to the transformations from amorphous to metastable fcc and from fcc to the stable hcp phases were observed in thin films in the ranges of 145-190 and 205-230°C, respectively. These phase transitions correlate with the drops of the films resistivity.

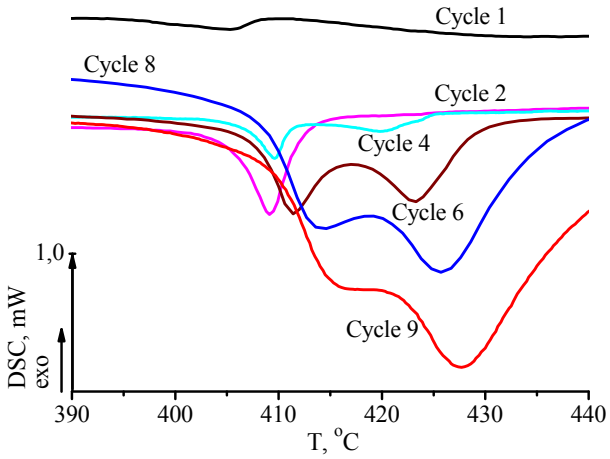

Fig. 9. Splitting of the endothermic peak for the GST225 thin film sample after multiple measurements.

Atomic-force microscopy showed that heat treatment of thin films is accompanied by the drastic morphology reconstruction. The mean height of the morphology increased from 1 to 42 nm for as-deposited and annealed at the temperature of 415°C films, respectively. Moreover, holes were observed for the sample treated at 485°C.

Existence of reproducible endothermic peak in the range of 390-415°C was revealed both for bulk GST225 and thin films. Following DSC measurements of the thin film sample showed that the value of endothermic peak sharply increased up to the third scanning, after which slowing was observed. For the bulk GST225 this peak became noticeable only after the third scanning, and then steadily increased.

Origin of endothermic peak is supposed to consist in the phase separation in the grains, due to the diffusion of the mobile Te atoms to the boundaries, which leads to strong inhomogeneity in composition of the grains. In this case the most probable reason for peak appearance is melting of $Ge_{18}Te_{82}$ eutectic mixture. Revealed process can initiate reliability issue in the phase-change memory devices, and require further careful investigation.

Acknowledgements

This study was supported by RFBR (project 08-03-00651) and the Target Programs of Basic Research of the Presidium of the RAS and the Division of Chemistry and Materials Science of the Russian Academy of Sciences.

We are grateful to Prof. Dobrochotova (IGIC RAS) for her help and for TG measurements.

References

[1] N. Yamada, E. Ohno, K. Nishiuchi, N. Akahira, M. Takao, J. Appl. Phys. **69**, 2849 (1991).
[2] S. Hudgens, B. Johnson, MRS Bulletin. **11**, 1 (2004).
[3] A. Pirovano, A.L. Lacaita, A. Benvenuti, F. Pellizzer, R. Bez, IEEE Transactions on Electron Devices, **51**, 452 (2004).
[4] A. L. Lacaita, Solid-State Electronics, **50**, 24 (2006).
[5] J. Akola, R. O. Jones, Phys. Rev. B**76**, 235201 (2007).
[6] Y. Fukuyama, N. Yasuda, J. Kim, H. Murayama, Y. Tanaka, S. Kimura, K. Kato, S. Kohara, Y. Moritomo, T. Matsunaga, R. Kojima, N. Yamada, H. Tanaka, T. Ohshima, M. Takata, Appl. Phys. Express 1 (2008) 045001.
[7] I. Friedrich, V. Weidenhof, W. Njoroge, P. Franz, M. Wuttig, J. Appl. Phys. **87**, 4130 (2000).
[8] S. R. Ovshinsky, Phys. Rev. Lett. **21**, 1450 (1968).
[9] E. J. Evans, J. H. Helbes, S. R. Ovshinsky, J. Non-Cryst. Solids. **2**. 334 (1970).
[10] J. Feinleib, J. de Neufville, S. C. Moss, S. R. Ovshinsky, Appl. Phys. Lett. **18**, 254 (1971).
[11] S. Privitera, C. Bongiorno, E. Rimini, R. Zonca, in Materials for Information Technology. Devices, Interconnections and Packaging, edited by E. Zschech, C. Whelan and T. Mikolajick (Springer, 2005) p. 189.
[12] N. Kh. Abrikosov, G. T. Danilova-Dobryakova, Izv. Akad. Nauk. SSSR Neorg. Mater. **1**, 204 (1965).
[13] A. V. Kolobov, R. Fons, A. I. Frenkel, A. L. Ankudinov, J. Tominaga, T. Uruga: Nat. Mater. **3,** 703 (2004).
[14] A. Pirovano, A.L. Lacaita, A. Benvenuti, F. Pellizzer, S. Hudgens, R. Bez, IEDM Tech. Dig. 699 (2003).
[15] N. Yamada, T. Matsunaga, J. Appl. Phys. **88**, 7020 (2000).

[16] Z. Sun, J. Zhou, R. Ahuja, Phys. Rev. Lett. **96**, 055507 (2006).
[17] C. Cabral Jr., K. N. Chen, L. Krusin-Elbaum, V. Deline, Appl. Phys. Lett. **90**, 051908 (2007).
[18] J. K. Olson, H. Li, P.C. Taylor, Journal of Ovonic Research **1**, 1 (2005).
[19] L. Krusin-Elbaum, C. Cabral,Jr., K. N. Chen, M. Copel, D. W. Abraham, K. B. Reuter, S. M. Rossnagel, J. Bruley, V. R. Deline, Appl. Phys. Lett. **90**, 141902 (2007).
[20] S. Privitera, C. Bongiorno, E. Rimini, R. Zonca, A. Pirovano, and R. Bez, in Advanced Data Storage Materials and Characterization Techniques, edited by J. W. Ahner, J. Levy, L. Hesselink, and A. Mijiritskii (Mater. Res. Soc. Symp. Proc. **803**, Warrendale, PA, 2004) p. 83.
[21] K. N. Chen, L. Krusin-Elbaum, C. Cabral Jr., C. Lavoie, J. Sun, S. Rossnagel, Non-Volatile Semiconductor Memory Workshop (2006) IEEE NVSMW, P.97-98.
[22] T. P. Leervard Pedersen *et al*, Appl. Phys. Lett. **79**, 3597 (2001).
[23] V. I. Kosyakov, V. A. Shestakov, L. E. Shelimova, F. A. Kuznetsov, V. S. Zemskov, Inorganic Materials, V.36, N10 (2000) P. 1004-1017.
[24] K. N. Chen, C. Cabrai Jr., L. Krusin-Elbaum, E-MRS Spring Meeting 2008. H11.
[25] J. Kalb, F. Spaepen, M. Wuttig, J. Appl. Phys., **93**, 2389 (2003).
[26] D. Ielmini, Y. Zhang, Appl. Phys. Lett. **90**, 192102 (2007).
[27] H. E. Kissinger, Anal.Chemie. **29**, 1702 (1957).
[28] T. H. Jeong, M. R. Kim, H. Seo, S. J. Kim, S. Y. Kim, J. Appl. Phys. **86**, 774 (1999).
[29] H. Seo, T.-H. Jeno, J.-W. Park, Ch. Yeon, S.-J. Kim, S.-Y. Kim, Jpn. J. Appl. Phys. **39,** 745 (2000).
[30] T. Zhang, B. Liu, Z.-T. Song, W.-L. Liu, S.-L. Feng, B. Chen, Chin. Phys. Lett. **22**, 1803 (2005).
[31] M. A. Paesler, D. A. Baker, G. Lucovsky, P. C. Taylor, J. S. Washington, J. Optoelectron. Adv. Mater. **9**, 2996 (2007).
[32] N. Kh. Abrikosov, V. F. Bankina *et al*, in Chalcogenide semiconductors and alloys on their basis, Nauka, Moscow (USSR) (1975).
[33] M. Hansen, K. Anderko. Constitution of binary alloys. NY, Toronto, London. McGraw Hill Book Co. (1958).

*Corresponding author: sergkoz@igic.ras.ru